N62-71226

NASA TN D-931

NASA TN D-931

IN-02
386827

TECHNICAL NOTE

D-931

EXPERIMENTAL AND THEORETICAL DEFLECTIONS AND NATURAL FREQUENCIES OF AN INFLATABLE FABRIC PLATE

By W. Jefferson Stroud

Langley Research Center
Langley Field, Va.

NATIONAL AERONAUTICS AND SPACE ADMINISTRATION

WASHINGTON October 1961

NATIONAL AERONAUTICS AND SPACE ADMINISTRATION

TECHNICAL NOTE D-931

EXPERIMENTAL AND THEORETICAL DEFLECTIONS AND NATURAL FREQUENCIES OF AN INFLATABLE FABRIC PLATE

By W. Jefferson Stroud

L
1
3
1
7

SUMMARY

Static and vibration tests were performed on an inflatable square fabric plate supported on all edges. Lateral deflections and natural frequencies showed good agreement with calculations made using a linear small-deflection theory.

INTRODUCTION

A structural concept which is being utilized for satellites and being considered for reentry vehicles is that of the inflatable structure. Packageability and automatic erectability make inflatable construction especially attractive for satellites and space stations. Inflatable construction may also provide a suitable means of building reentry vehicles with low wing loadings in order to alleviate the problem of reentry heating.

For these applications information is needed on the load-carrying capabilities and structural characteristics of inflatable structures. Simple methods of analysis have been used successfully for determining collapse loads for certain types of inflated structures (refs. 1 and 2); however, for detailed study of stresses, deflections, vibration modes and frequencies, and so forth, applications of more refined structural theory may be necessary. An example of inflated construction which might be useful as the structure of an inflated reentry glider is an inflated fabric plate called Airmat. Airmat, which was developed by Goodyear Aircraft Corporation, consists of two covers of coated woven material connected by closely spaced flexible fibers called drop cords (fig. 1). A theory for the structural analysis of inflatable fabric plates, such as Airmat, has been presented in detail in reference 3. The purpose of this investigation is to assess the validity of the theory of reference 3 by comparing experimental static deflections and natural frequencies of an inflatable fabric plate with the results of calculations made with this theory.

SYMBOLS

$$A_{11} = \frac{E_W t}{1 - \mu_{WF}\mu_{FW}}$$

$$A_{12} = \frac{\mu_{FW}E_W t}{1 - \mu_{WF}\mu_{FW}}$$

$$A_{21} = \frac{\mu_{WF}E_F t}{1 - \mu_{WF}\mu_{FW}}$$

$$A_{22} = \frac{E_F t}{1 - \mu_{WF}\mu_{FW}}$$

$$A_{33} = Gt$$

a,b	length of rectangular plate in x- and y-directions, respectively
$E_W t$	extensional stiffness in warp direction of cover
$E_F t$	extensional stiffness in fill direction of cover
Gt	shear stiffness of cover
g	structural damping factor
h	depth of plate
m,n	number of half waves in x- and y-directions, respectively
p	difference between external pressure and internal pressure in inflatable fabric plate
q	uniformly distributed external loading per unit area
t	thickness of one cover
w	lateral deflection of plate
w_c	lateral deflection at center of plate

L
1
3
1
7

x,y,z	rectangular Cartesian coordinate system
λ	length-width ratio of plate
μ_{WF}	Poisson's ratio associated with a contraction in the fill direction caused by a tensile stress in the warp direction
μ_{FW}	Poisson's ratio associated with a contraction in the warp direction caused by a tensile stress in the fill direction
ρ	mass of plate per unit middle plane area
ω	frequency

TEST SPECIMEN

Tests were performed on the inflatable fabric plate specimen shown in figure 2. The specimen was 18 inches square with a 2-inch mounting flange and had a constant depth of $1\frac{1}{8}$ inches. Each cover of the plate was made of two layers of woven nylon with nylon drop cords interwoven into the inner layer. The threads of the two layers were oriented in the same directions and were bonded and coated with neoprene to make the plate airtight. This nylon-neoprene fabric carries the Goodyear Aircraft Corporation designation number XA27A209.

The valves located near the corners were used to inflate the plate and measure the internal pressure. In order to seal the edges of the plate an additional sheet of woven material was glued to the surface of the plate at the edge and extended to help form the 2-inch flange around the plate. The valves and extra material glued to the surface of the plate represent departures from uniformity which could not be readily accounted for in the theory of reference 3. Another factor not accounted for in the theory is the roundness of the plate edges and corners.

STATIC TESTS

Static tests were conducted on the inflatable fabric plate in order to obtain the deflectional behavior of the specimen. These tests consisted of measuring the lateral deflection of the specimen caused by an external uniformly distributed loading for various internal pressures.

Test Apparatus and Procedure

Figure 3 is a schematic drawing of the test setup for the static tests. The inflatable fabric plate was attached to the top of a loading tank by using the two types of supporting fixtures shown in figure 4. In one case (fig. 4(a)) the 2-inch flange around the plate was attached to the fixture so as to simulate simple support. In the other case (fig. 4(b)) a plywood frame was used to move the effective plate boundary inside the reinforced region along the boundary of the plate and, at the same time, to simulate clamped-boundary conditions. Figures 5 and 6 are photographs of the plate mounted in the plywood clamped-boundary fixture showing deflection measuring apparatus and pressure-regulating and pressure-measuring equipment.

L
1
3
1
7

In all cases when the clamped-boundary fixture was used, the test procedure followed was designed to permit, as nearly as possible, a free buildup of inplane stresses due to internal pressure. The wooden strip noted in figure 4(b) was glued to the surface of the plate with rubber cement. With each change of internal pressure this seal was broken and the clamped boundary released. The plate was reclamped and resealed after the desired pressure was attained.

The loading on the specimen was applied by pressurizing the airtight tank over which the specimen was bolted. The loading increments were approximately 1 psfg. The regulating system used to obtain these relatively small loading increments from a 100 psi supply consisted of two regulators in series with an orifice, expansion tank, and needle valve. The loading pressure was measured with a Magnehelic diaphragm pressure gage. The internal pressure in the plate was controlled with a regulator and measured with a mercury manometer. Figures 3 and 6 illustrate the pressure regulating and measuring apparatus.

Deflection measurements were made with a dial gage (figs. 3 and 5). The spring force of the dial gage was sufficiently large to influence the deflection of the specimen significantly; therefore, this force had to be eliminated for these tests. The elimination of the dial-gage force was accomplished by fitting the dial gage with a screw with which the extension of the gage spindle could be adjusted until it just touched the surface of the plate. Contact was detected by an electric circuit which activated an electron-ray tube. This technique is similar to that described in reference 4.

Results and Discussion

Simply supported plate.- Results of the static tests made with the use of the simple-support boundary conditions are compared with theoretical results in figure 7. Values of the deflection parameter w_c/h, where w_c is the deflection at the center of the plate and h is the plate depth, are plotted against the loading for three values of internal pressure of the plate. The theory is presented as solid lines and the test-point symbols represent experimental values. The theoretical deflections are given by equation (A1) of the appendix with the following values of material constants: $A_{11} = 971$ pounds per inch, $A_{22} = 716$ pounds per inch, $A_{12} = A_{21} = 124$ pounds per inch, and $A_{33} = 100$ pounds per inch. These constants are typical values found in static materials tests made on the cover fabric. (See ref. 2.) At low internal pressures, accurate material constants are not essential because most of the deflection is caused by transverse shear which is not affected by these constants. For example, at an internal pressure of 5.3 psig, corresponding to the upper curve in figure 7, 82 percent of the theoretical deflection of the specimen is shear deflection.

The agreement between test results and theoretical results is seen to be good. The double-thick reinforced region near the plate boundary can be expected to be stiffer than the remainder of the plate. Since this extra stiffness is not accounted for in the theory, it might be expected that the theory would yield slightly higher center deflections than the tests. It appears, however, that the discrepancies noticeable in figure 7 may be partly due to nonlinearity associated with large deflections. (The limit of applicability of the linear theory is investigated briefly in ref. 3.)

Clamped plate.- Results of the static tests made with the clamped boundary are compared with theoretical results in figure 8. As in the simple-support case, values of the center deflection parameter w_c/h are plotted against the loading for three values of internal pressure. The theory is shown as solid lines and the test-point symbols represent experimental values. The theoretical calculations were made by using equation (A2) of the appendix, with the constants A_{11}, A_{12}, A_{21}, and A_{33} having the same values as in the simple-support case. These results, consistent with the smaller deflections obtained, are more nearly linear than the simple-support results.

The agreement between theory and experiment is very good except at an internal pressure of 14 psig. The reason for the discrepancy at this pressure is not known but may be associated with boundary restraint of free expansion of the plate on pressurization, which could not be completely eliminated at this internal pressure by the technique employed.

For the clamped boundary, transverse shear deflections are even more important than for the simple-support boundary. For example, with a clamped boundary at an internal pressure of 15 psig, about 91 percent of the total calculated deflection is shear deflection and, at an internal pressure of 5 psig, about 97 percent of the total deflection is shear deflection.

VIBRATION TESTS

Vibration tests were performed on the inflatable fabric plate to obtain the lower modes and frequencies. As in the static tests both the simple-support boundary and the clamped boundary were used. A value of the structural damping factor for the first vibration mode was obtained experimentally for the simple-support boundary only.

L
1
3
1
7

Test Appratus and Procedure

The equipment used in the vibration tests consisted of a pulsating air-jet shaker (ref. 5), a manual response pickup, and a response indicating and recording system. (See fig. 9.) Because of the flexibility of the woven covers of the plate, it was necessary to use a probe-type velocity pickup with a very small spring force - 2 pounds per inch. For the low frequencies the signal from this pickup was fed into an amplifier and recording system. Frequencies were obtained from the graphical records. Above 33 cps the pickup signal was fed into a Stroboconn frequency indicator from which frequencies could be read directly. A cathode-ray oscilloscope was used to survey the vibration phase relationships across the plate to determine the location of node lines.

As one means of obtaining the structural damping factor in the first mode, an amplitude-frequency response curve was plotted for the center of the simply supported plate. The amplitude of vibration at the center of the plate was determined by using the deflection-measuring technique described in the static tests. The dial-gage spindle was screwed down until first contact was made with the plate at its maximum vertical displacement. Contact was ascertained by the blinking of the electron-ray tube. An alternate determination of first-mode damping was also made by measuring the rate of amplitude decay at the center of the plate when the exciting force was removed. This measurement was made with the velocity pickup in a fixed mount and the output was recorded graphically.

Results and Discussion

Simply supported plate.- In figure 10 the frequency results of the vibration tests on the simply supported plate are compared with theoretical results obtained by using equation (A4) of the appendix. In order to make the theoretical calculations, values of the material constants A_{11}, A_{12}, A_{21}, A_{22}, and A_{33} were required. Appropriate values for dynamic conditions may be significantly different from the appropriate values for static conditions. However, in lieu of dynamic material data for the nylon-neoprene fabric material, the static values for the constants were used in these calculations.

Theoretical results for frequency are presented as solid lines in figure 10 and the test-point symbols represent experimental values. The numbers adjacent to the curves identify the modes according to the number of half waves in each direction. The small sketches at the right represent the nodal patterns associated with each of the modes as obtained in the tests. Because the plate material is woven and has different properties in the warp and fill directions, certain modes, which in an isotropic plate would have identical frequencies, have two distinct frequency curves depending on the direction of the node lines. Notice, for example, the frequency curves for the 1,2 and 2,1 modes and the 1,3 and 3,1 modes. The slanting of the node lines indicated for most cases was caused by the two valves in the corners. The material in these regions was stiffer and heavier than the plate material proper and tended to pull the node lines toward the valves. Note that no results are shown for modes with two node lines in one direction and one in the other direction. Although frequencies can be calculated for such modes, they were not found experimentally. The maximum difference between theoretical and experimental frequencies for the simple-support boundary was 11 percent.

L
1
3
1
7

The experimental amplitude-response curve for the first mode vibration of the simply supported plate is shown in figure 11. The test-points which established the curve are shown by the circles. Characteristics of the response curve which are pertinent to the determination of the structural damping factor (see, for example, refs. 6 and 7) are indicated in the plot. The corresponding value of the structural damping factor was calculated to be $g = 0.035$ at 9.4 psig internal pressure. This value was verified by the measured rate of amplitude decay of free vibration.

<u>Clamped plate</u>.- In figure 12 the results of the vibration tests on the clamped plate are compared with theoretical results calculated by means of equations (A6) to (A8) and (A10) of the appendix. As in the frequency calculations for the simply supported plate, the static material constants were used. The theoretical results are shown by the solid curves. Certain approximations involved in obtaining these calculated results are discussed in the appendix. The experimental results are shown by the test-point symbols, and nodal patterns are indicated again by the small sketches at the right. As in the vibration tests with the simple-support boundary, some of the modes indicated by the theory were not found experimentally.

The effect of the valves on the nodal patterns was less pronounced for the clamped plate than for the simply supported plate because the boundary was moved in so that the valves were located nearer the boundary for the clamped plate. The maximum difference in frequency between theory and experiment in the vibration tests of the clamped plate was 13 percent.

CONCLUDING REMARKS

L

Results from static and vibration tests on an inflatable square 1
fabric plate specimen are compared with calculations made by using a 3
recently developed linear theory for inflatable plates in order to 1
assess the validity of the theory. Agreement for both static deflec- 7
tions and frequencies was good even though certain features of the test specimen were not accounted for in the theory. Transverse shear deflections were important particularly for the clamped-boundary condition. Damping for first mode vibration of the simply supported plate was investigated and found to be fairly low; a structural damping factor of about 0.035 at an internal pressure of 9.4 psig was obtained.

Langley Research Center,
National Aeronautics and Space Administration,
Langley Field, Va., May 25, 1961.

APPENDIX

EQUATIONS FOR INFLATABLE PLATE DEFLECTIONS AND FREQUENCIES

Static Deflection

Simply supported plate.- The static deflection of a simply supported inflatable plate subject to a uniform lateral load q was found in reference 3 to be given by

$$w = \sum_{m=1,3,\cdots}^{\infty} \sum_{n=1,3,\cdots}^{\infty} w_{mn} \sin \frac{m\pi x}{a} \sin \frac{n\pi y}{b} \tag{A1}$$

where

$$w_{mn} = \frac{R\bar{q}h}{mn\left\{\left(1 - \frac{R^2\bar{p}^2}{4\Lambda_{mn}}\right)a_{mn} - \frac{R\bar{p}}{2\Lambda_{mn}}\left[e_{mn} + \left(\lambda^2 m^2 - n^2\right)^2 \bar{A}_{33}\right]\right\}}$$

with

$$\bar{q} = \frac{4q}{\pi^2 p}$$

$$R = \frac{4b^2}{\pi^2 h^2}$$

$$\bar{p} = \frac{ph}{A_{11}}$$

$$\Lambda_{mn} = \frac{1}{4}\left[\left(R\bar{p} + b_{mn}\right)\left(R\bar{p} + c_{mn}\right) - d_{mn}{}^2\right]$$

$$\lambda = \frac{b}{a}$$

$$a_{mn} = \lambda^2 m^2 + n^2$$

$$b_{mn} = 2\left(\lambda^2 m^2 + \bar{A}_{33} n^2\right)$$

$$c_{mn} = 2\left(\bar{A}_{22} n^2 + \bar{A}_{33} \lambda^2 m^2\right)$$

$$d_{mn} = 2\lambda mn\left(\bar{A}_{12} + \bar{A}_{33}\right)$$

$$e_{mn} = \lambda^2 m^2 n^2 \left(1 + \bar{A}_{22} - 2\bar{A}_{12}\right)$$

L
1
3
1
7

and where

$$\bar{A}_{12} = \frac{A_{12}}{A_{11}}$$

$$\bar{A}_{22} = \frac{A_{22}}{A_{11}}$$

$$\bar{A}_{33} = \frac{A_{33}}{A_{11}}$$

In the calculation of the center deflections shown in figure 7, four terms were retained in equation (A1). The contribution of the remaining terms was negligible.

Clamped plate.- The static deflection of a clamped inflatable plate (ref. 3) is given by

$$w = \sum_{m=1}^{\infty} \sum_{n=1}^{\infty} w_{mn} \sin \frac{m\pi x}{a} \sin \frac{n\pi y}{b} \tag{A2}$$

where a first approximation with terms corresponding to $m = 1, 2$ and $n = 1, 2$ leads to

$$w_{11} = \frac{R\bar{q}h}{\left(1 - \frac{16}{9\pi^2}\frac{R^2\bar{p}^2}{\Lambda}\right)a_{11} - \frac{16}{9\pi^2}\frac{R\bar{p}}{\Lambda}\left(\lambda^2 c_{12} + b_{21} - \frac{32}{9\pi^2}\lambda d_{22}\right)}$$

and

$$w_{12} = w_{21} = w_{22} = 0$$

In addition to symbols already defined,

$$\Lambda = \frac{1}{4}\left[\left(R\bar{p} + b_{21}\right)\left(R\bar{p} + c_{12}\right) - \left(\frac{16d_{22}}{9\pi^2}\right)^2\right]$$

Vibration Frequencies

Simply supported plate.- In reference 3 the lateral deflection modes of vibration of the simply supported plate are found to have exactly the form

$$w = \bar{w}_{mn}e^{i\omega t} \sin \frac{m\pi x}{a} \sin \frac{n\pi y}{b} \tag{A3}$$

where $\bar{w}_{mn}$ is the amplitude of the m,n component and the frequencies ω correspond to the solutions of the equation

$$k^6 - \left[\bar{p}\left(2R + a_{mn}\right) + b_{mn} + c_{mn}\right]k^4 + \left[\bar{p}^2R\left(R + a_{mn}\right) + \bar{p}\left(R + a_{mn}\right)\left(b_{mn} + c_{mn}\right)\right.$$

$$\left. + \left(b_{mn}c_{mn} - d_{mn}^2\right)\right]k^2 - \bar{p}^2Rf_{mn} - \bar{p}a_{mn}\left(b_{mn}c_{mn} - d_{mn}^2\right) = 0 \tag{A4}$$

where, in addition to quantities already defined,

$$k^2 = \frac{\rho\omega^2b^2}{A_{11}\pi^2}$$

and

$$f_{mn} = \lambda^2 m^2 b_{mn} + n^2 c_{mn} + 2\lambda mn\, d_{mn}$$

Clamped plate.- In reference 3, the lateral deflection w of each natural vibration mode of the clamped plate was approximated by the series

$$w = \sum_{m=1}^{M} \sum_{n=1}^{N} \bar{w}_{mn} e^{i\omega t} \sin \frac{m\pi x}{a} \sin \frac{n\pi y}{b} \tag{A5}$$

L
1
3
1
7

The first three frequency curves in figure 12 have been obtained by setting $M = N = 2$; thus four terms of the series in equation (A5) are retained.

The lowest mode is given by the solution of the equation

$$\begin{vmatrix} \frac{\pi^2 h}{b}\left[k^2 - \bar{p}\left(\lambda^2 + 1\right)\right] & -\frac{8}{3}\bar{p}\lambda & -\frac{8}{3}\bar{p} \\ -\frac{8}{3}\bar{p}\lambda & \frac{\pi^2 h}{4b}k^2 - \frac{\bar{p}b}{h} - \frac{\pi^2 h}{2b}\left(4\lambda^2 + \bar{A}_{33}\right) & -\frac{32}{9}\frac{h}{b}\lambda\left(\bar{A}_{12} + \bar{A}_{33}\right) \\ -\frac{8}{3}\bar{p} & -\frac{32}{9}\frac{h}{b}\lambda\left(\bar{A}_{12} + \bar{A}_{33}\right) & \frac{\pi^2 h}{4b}k^2 - \frac{\bar{p}b}{h} - \frac{\pi^2 h}{2b}\left(\lambda^2 \bar{A}_{33} + 4\bar{A}_{22}\right) \end{vmatrix} = 0 \tag{A6}$$

and corresponds to a mode shape such that

$$\bar{w}_{11} \neq 0$$

$$\bar{w}_{12} = \bar{w}_{21} = \bar{w}_{22} = 0$$

The second frequency curve results from the solution of

$$\begin{vmatrix} \frac{\pi^2 h}{b}\left[k^2 - \bar{p}\left(\lambda^2 + 4\right)\right] & -\frac{8}{3}\bar{p}\lambda & \frac{8}{3}\bar{p} \\ -\frac{8}{3}\bar{p}\lambda & \frac{\pi^2 h}{4b}k^2 - \frac{\bar{p}b}{h} - \frac{\pi^2 h}{2b}\left(4\lambda^2 + 4\bar{A}_{33}\right) & \frac{32}{9}\frac{h}{b}\lambda\left(\bar{A}_{12} + \bar{A}_{33}\right) \\ \frac{8}{3}\bar{p} & \frac{32}{9}\frac{h}{b}\lambda\left(\bar{A}_{12} + \bar{A}_{33}\right) & \frac{\pi^2 h}{4b}k^2 - \frac{\bar{p}b}{h} - \frac{\pi^2 h}{2b}\left(\lambda^2\bar{A}_{33} + \bar{A}_{22}\right) \end{vmatrix} = 0 \qquad \text{(A7)}$$

and corresponds to

L1317

$$\bar{w}_{12} \neq 0$$

$$\bar{w}_{11} = \bar{w}_{21} = \bar{w}_{22} = 0$$

The third frequency curve results from

$$\begin{vmatrix} \frac{\pi^2 h}{b}\left[k^2 - \bar{p}\left(4\lambda^2 + 1\right)\right] & \frac{8}{3}\bar{p}\lambda & -\frac{8}{3}\bar{p} \\ \frac{8}{3}\bar{p}\lambda & \frac{\pi^2 h}{4b}k^2 - \frac{\bar{p}b}{h} - \frac{\pi^2 h}{2b}\left(\lambda^2 + \bar{A}_{33}\right) & \frac{32}{9}\frac{h}{b}\lambda\left(\bar{A}_{12} + \bar{A}_{33}\right) \\ -\frac{8}{3}\bar{p} & \frac{32}{9}\frac{h}{b}\lambda\left(\bar{A}_{12} + \bar{A}_{33}\right) & \frac{\pi^2 h}{4b}k^2 - \frac{\bar{p}b}{h} - \frac{\pi^2 h}{2b}\left(4\lambda^2\bar{A}_{33} + 4\bar{A}_{22}\right) \end{vmatrix} = 0 \qquad \text{(A8)}$$

and corresponds to

$$\bar{w}_{21} \neq 0$$

$$\bar{w}_{11} = \bar{w}_{12} = \bar{w}_{22} = 0$$

Obviously, a curve exists corresponding to the mode for which

$$\bar{w}_{22} \neq 0$$

$$\bar{w}_{11} = \bar{w}_{12} = \bar{w}_{21} = 0$$

The corresponding frequency equation is

$$\begin{vmatrix} \frac{\pi^2 h}{b}\left[k^2 - \bar{p}\left(4\lambda^2 + 4\right)\right] & \frac{8}{3}\bar{p}\lambda & \frac{8}{3}\bar{p} \\ \frac{8}{3}\bar{p}\lambda & \frac{\pi^2 h}{4b}k^2 - \frac{\bar{p}b}{h} - \frac{\pi^2 h}{2b}\left(\lambda^2 + 4\bar{A}_{33}\right) & -\frac{32}{9}\frac{h}{b}\lambda\left(\bar{A}_{12} + \bar{A}_{33}\right) \\ \frac{8}{3}\bar{p} & -\frac{32}{9}\frac{h}{b}\lambda\left(\bar{A}_{12} + \bar{A}_{33}\right) & \frac{\pi^2 h}{4b}k^2 - \frac{\bar{p}b}{h} - \frac{\pi^2 h}{2b}\left(4\lambda^2\bar{A}_{33} + \bar{A}_{22}\right) \end{vmatrix} = 0 \qquad \text{(A9)}$$

This curve is not shown in figure 12 because the corresponding experimental mode was not clearly established.

For modes beyond the $\bar{w}_{22}$ mode, equation (A5) would have to be extended to include terms for which $m,n > 2$.

Consider the consequencies of arbitrarily retaining only one term in equation (A5), say, the term for which $m = 1$ and $n = 2$. In this approximation it can be shown (ref. 3) that rotation of the drop cords is not permitted to add to the lateral deflections due to shear. The resulting frequency equation corresponds to retention of only the term $\left[k^2 - \bar{p}\left(\lambda^2 + 4\right)\right]$ in equation (A7) and will yield a higher value of frequency than that obtained from equation (A7). Since shear flexibility is so important in inflatable plates, this pure shear approximation to the frequency may often be satisfactory. In fact, for the nylon-neoprene plate specimen, this one-term approximation is only 5 percent higher than that given by equation (A7) and shown in figure 12.

Note that the corresponding approximation for the third mode with only the terms for which $m = 2$ and $n = 1$ in equation (A5) being retained yields the same frequencies as the second mode. The second and third curves are thus replaced by a single curve because the difference between these two frequencies depends on the properties of the surface material which are not involved in pure shear deformation.

For the higher modes where shear deformation is even more important, the one-term approximation can be expected to be still better. For this reason, it has been used to calculate the higher frequency curves in figure 12. Thus, the upper three curves are given by the equation

$$k^2 = \bar{p}\left(\lambda^2 m^2 + n^2\right) \tag{A10}$$

where m,n are 1,3; 2,3; and 1,4, respectively.

REFERENCES

1. Leonard, Robert W., Brooks, George W., and McComb, Harvey G., Jr.: Structural Considerations of Inflatable Reentry Vehicles. NASA TN D-457, 1960.

2. Leonard, R. W., McComb, H. G., Jr., Zender, G. W., and Stroud, W. J.: Analysis of Inflated Reentry and Space Structures. Proc. of Recovery of Space Vehicles Symposium, Los Angeles, Calif., Aug. 31 - Sept. 1, 1960. (Sponsored by Inst. Aero. Sci. and Air Res. Dev. Command.)

3. McComb, Harvey G., Jr.: A Linear Theory for Inflatable Plates of Arbitrary Shape. NASA TN D-930, 1961.

4. Zender, George W., and Brooks, William H., Jr.: An Approximate Method of Calculating the Deformations of Wings Having Swept, M or W, Λ, and Swept-Tip Plan Forms. NACA TN 2978, 1953.

5. Herr, Robert W.: A Wide-Frequency-Range Air-Jet Shaker. NACA TN 4060, 1957.

6. Myklestad, N. O.: Vibration Analysis. McGraw-Hill Book Co., Inc., 1944, p. 111.

7. Soroka, Walter W.: Note on the Relations Between Viscous and Structural Damping Coefficients. Jour. Aero. Sci., vol. 16, no. 7, July 1949, pp. 409-410, 448.

L-1317

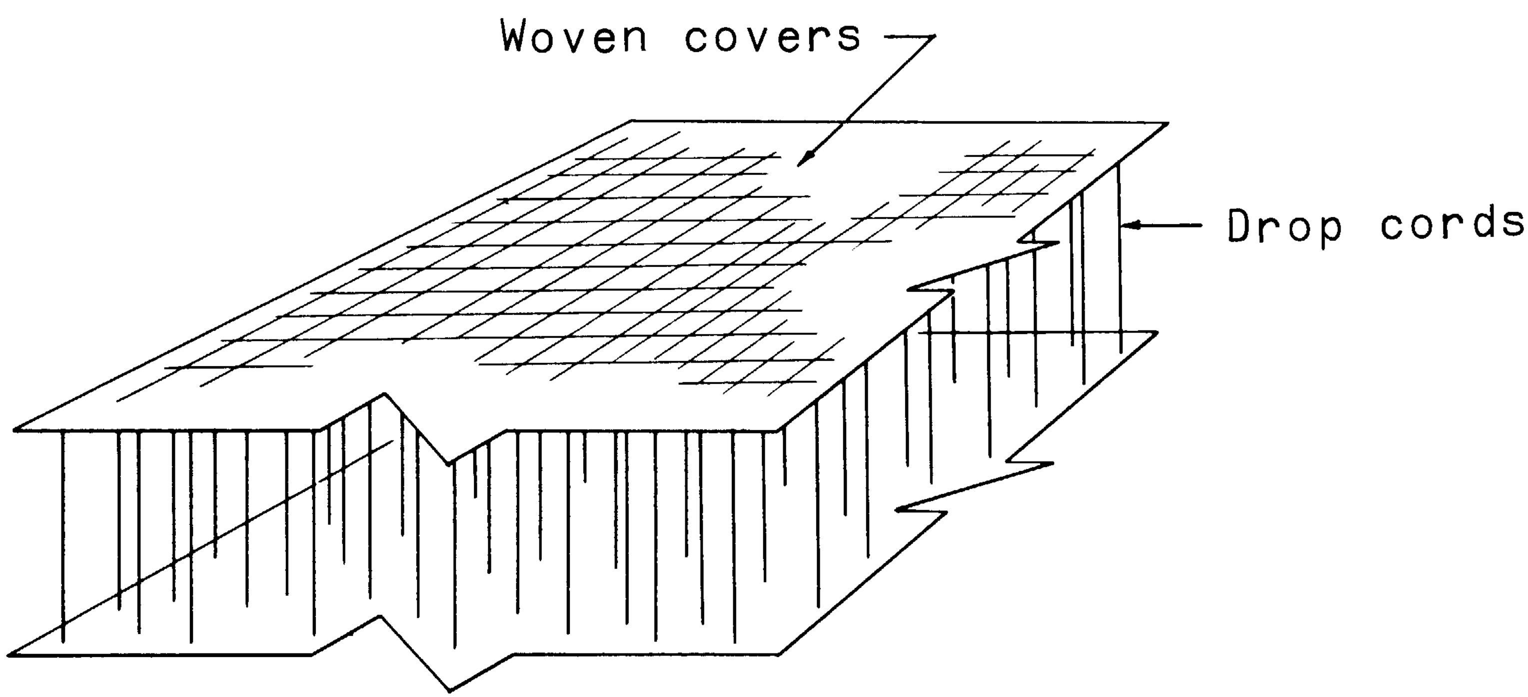

Figure 1.- Typical inflatable fabric plate construction.

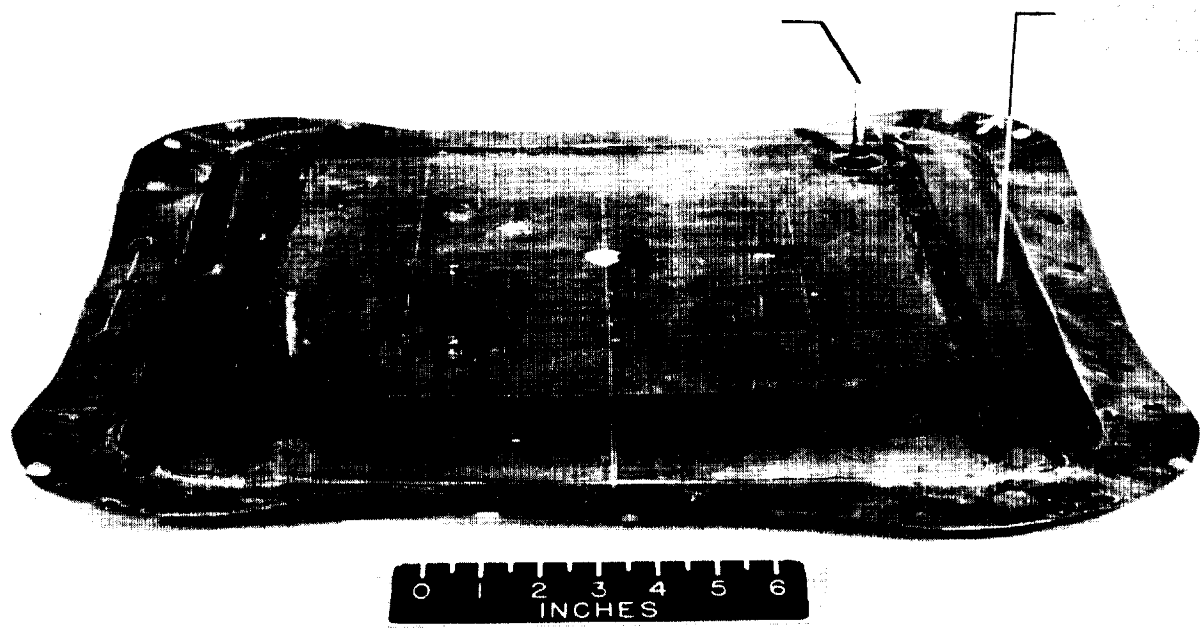

L-60-4018.1

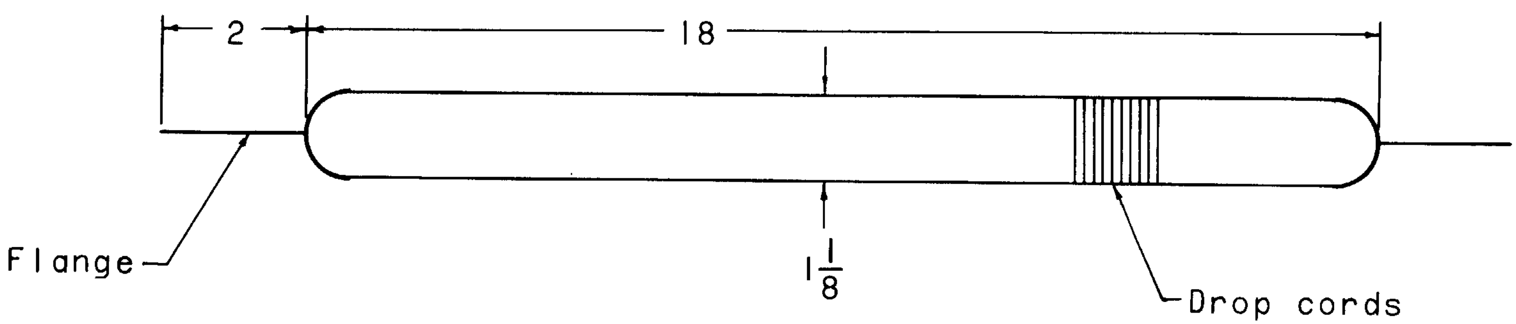

Figure 2.- Plate test specimen. All dimensions are in inches.

L-1317

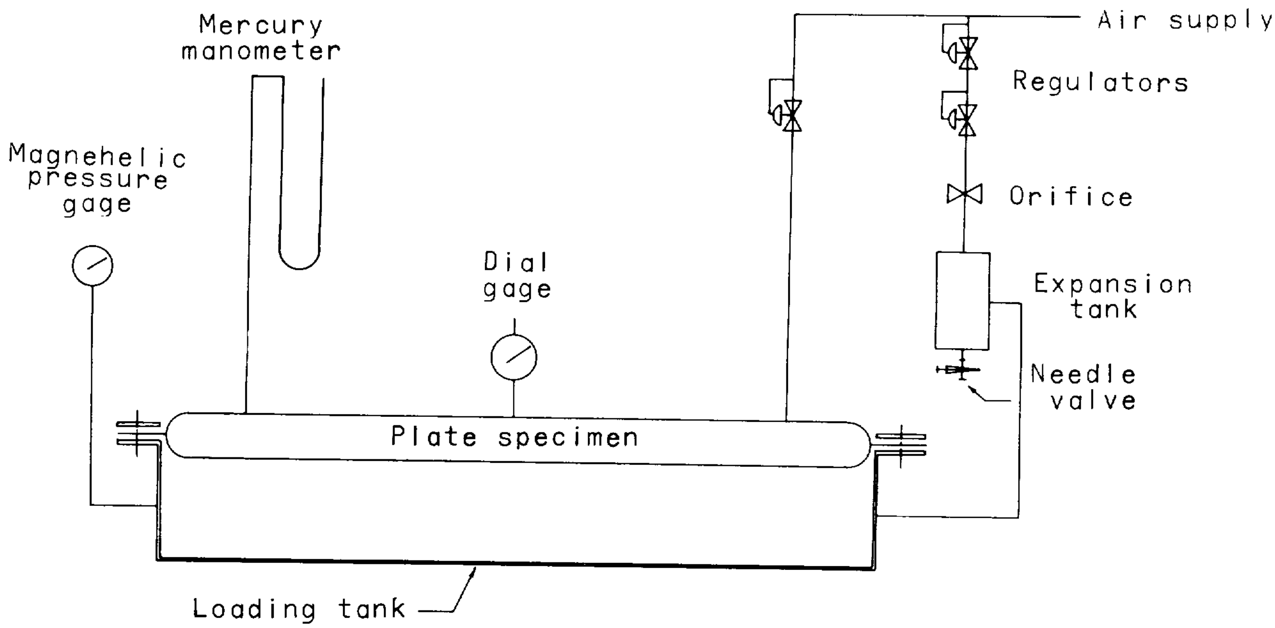

Figure 3.- Schematic diagram of static test setup.

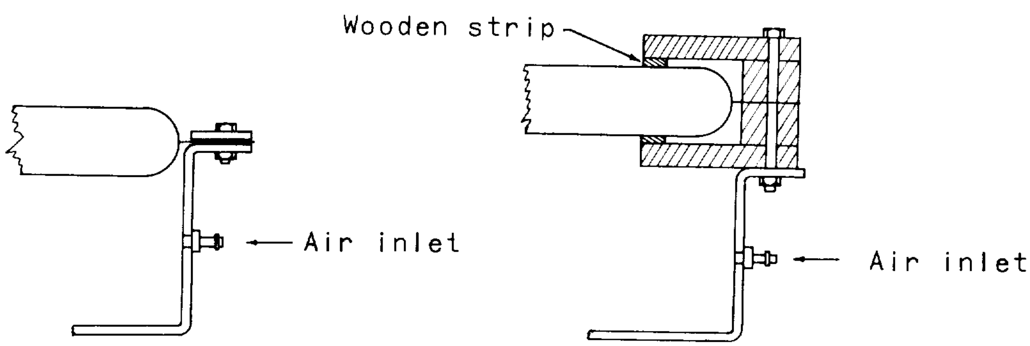

(a) Simple-support boundary.

(b) Clamped boundary.

Figure 4.- Details of supporting fixtures.

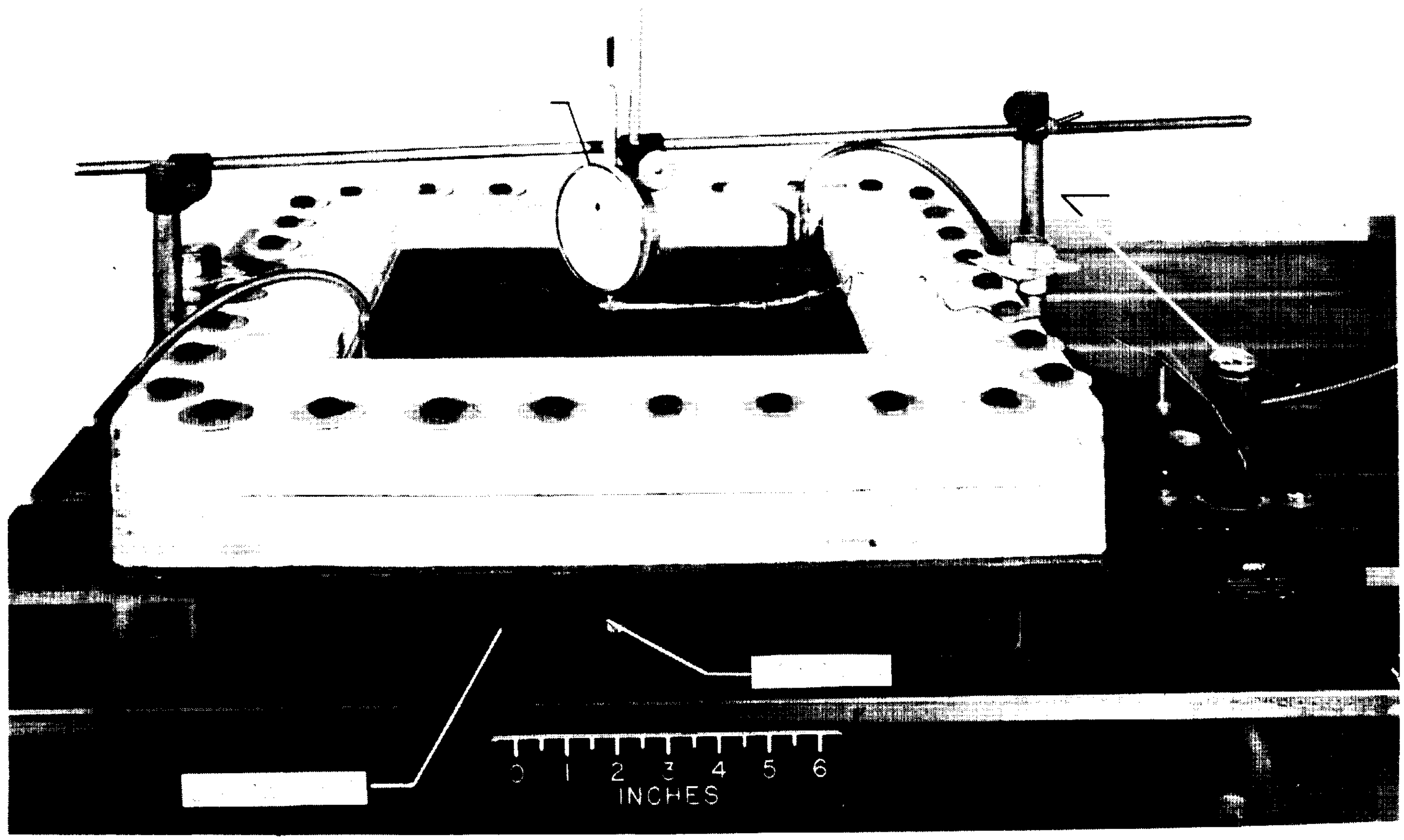

L-60-4017.1

Figure 5.- Plate in clamped boundary showing deflection-measuring apparatus (static tests).

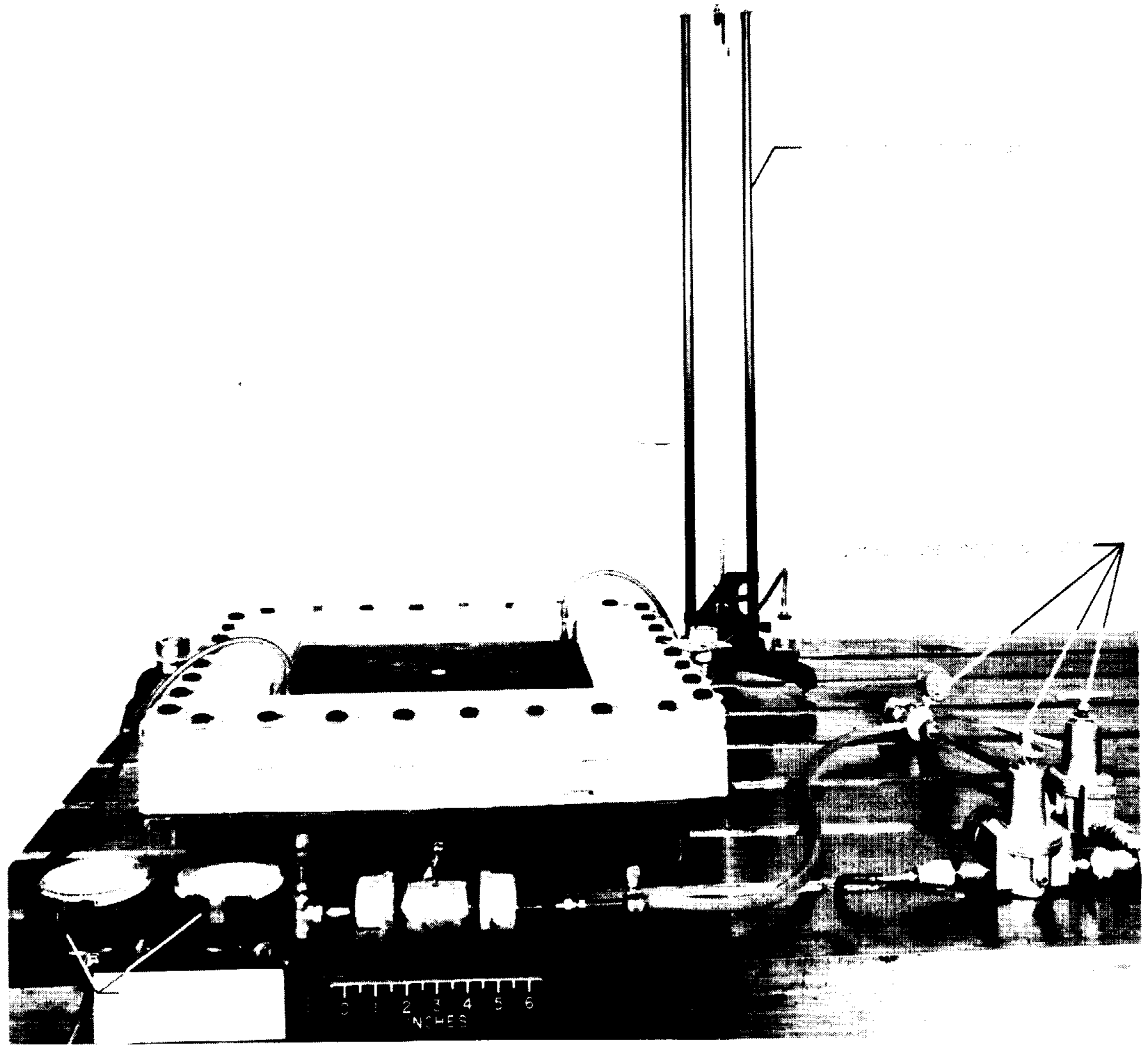

L-60-4016.1

Figure 6.- Plate in clamped boundary showing pressure-regulating and pressure-measuring apparatus (static tests).

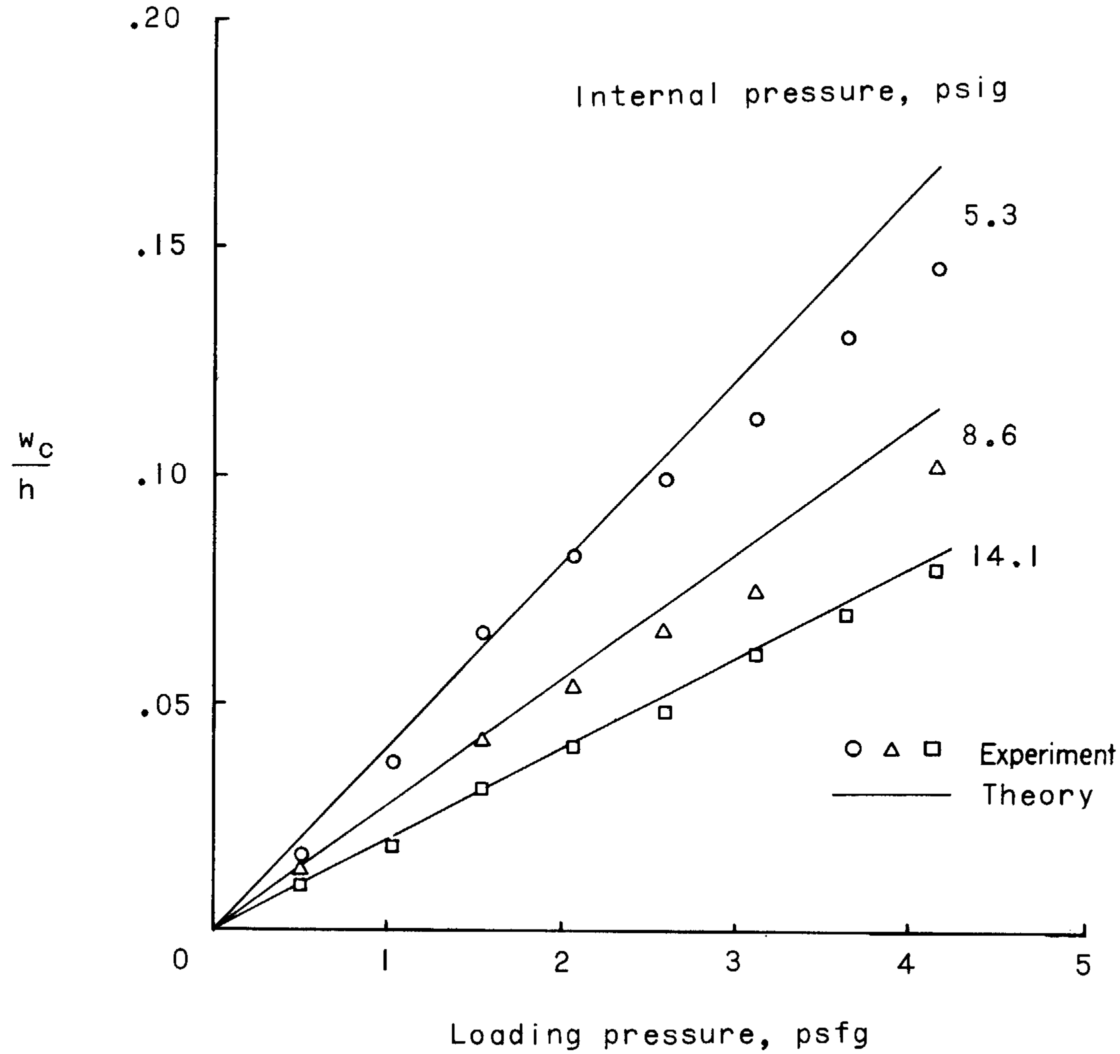

Figure 7.- Theoretical and experimental deflections plotted against load for a simply supported inflatable fabric plate with various values of internal pressure.

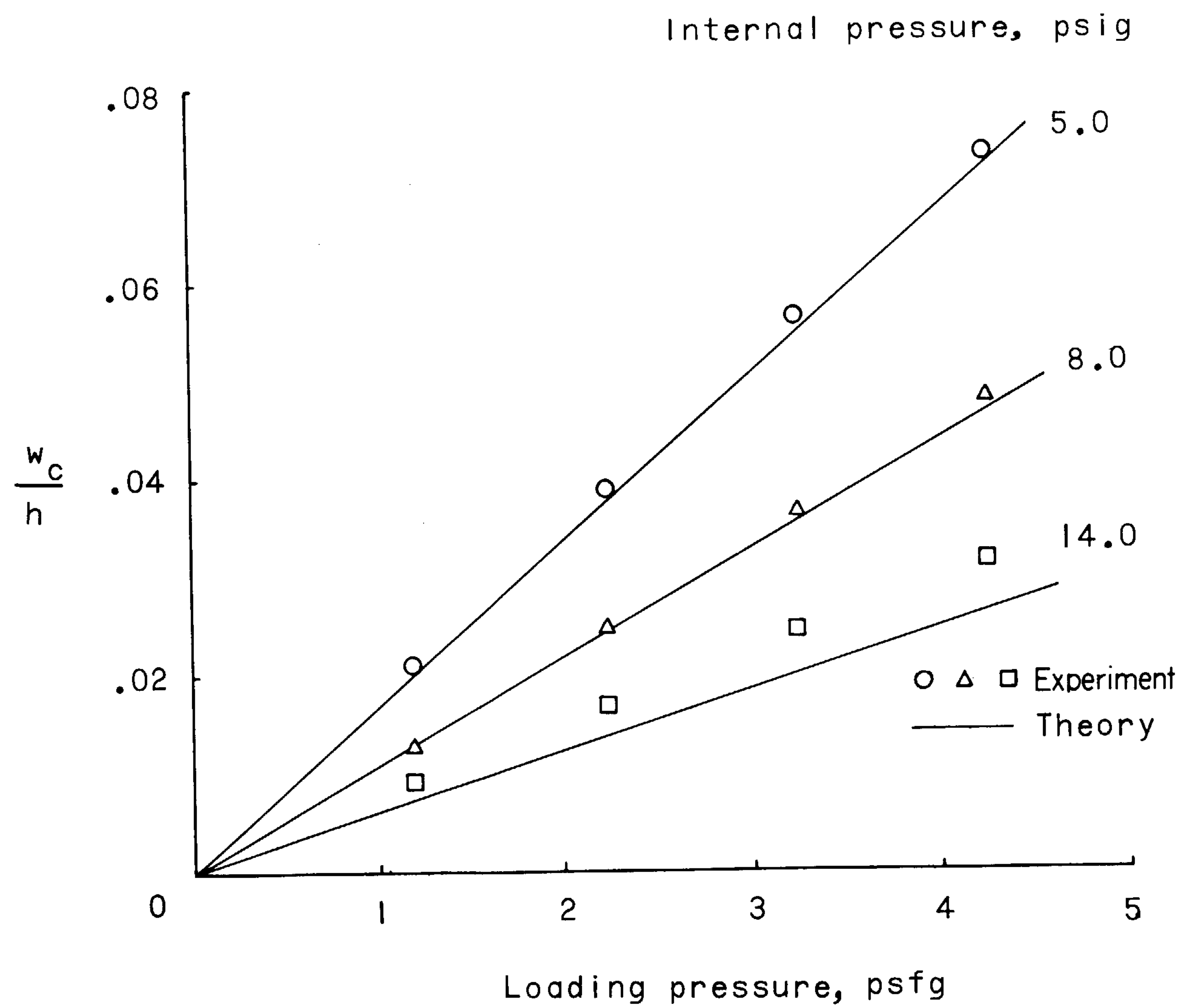

Figure 8.- Theoretical and experimental deflections plotted against load for a clamped inflatable fabric plate for various values of internal pressure.

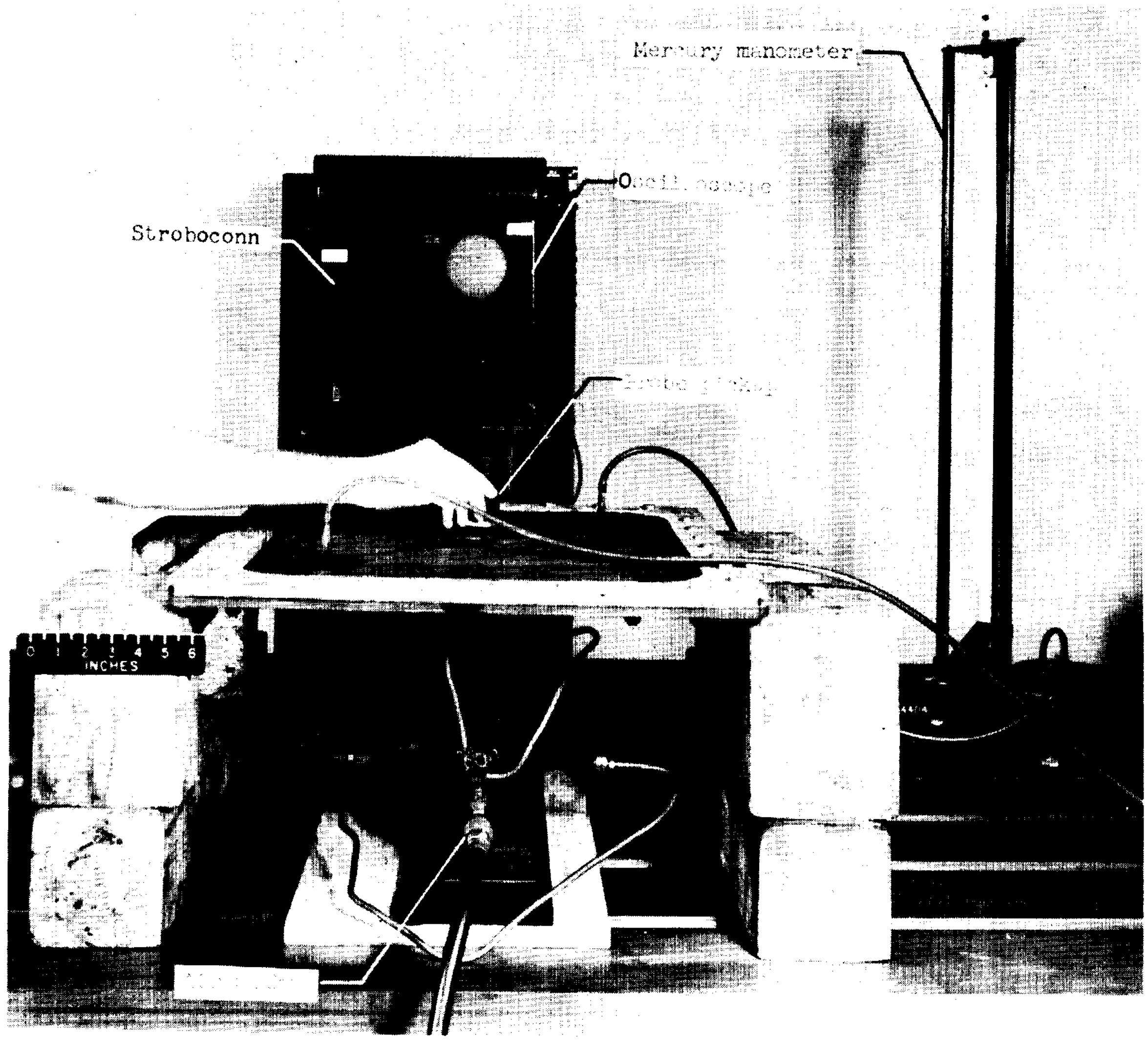

L-60-4482.1

Figure 9.- Plate in simple-support boundary showing vibration test setup.

L-1317

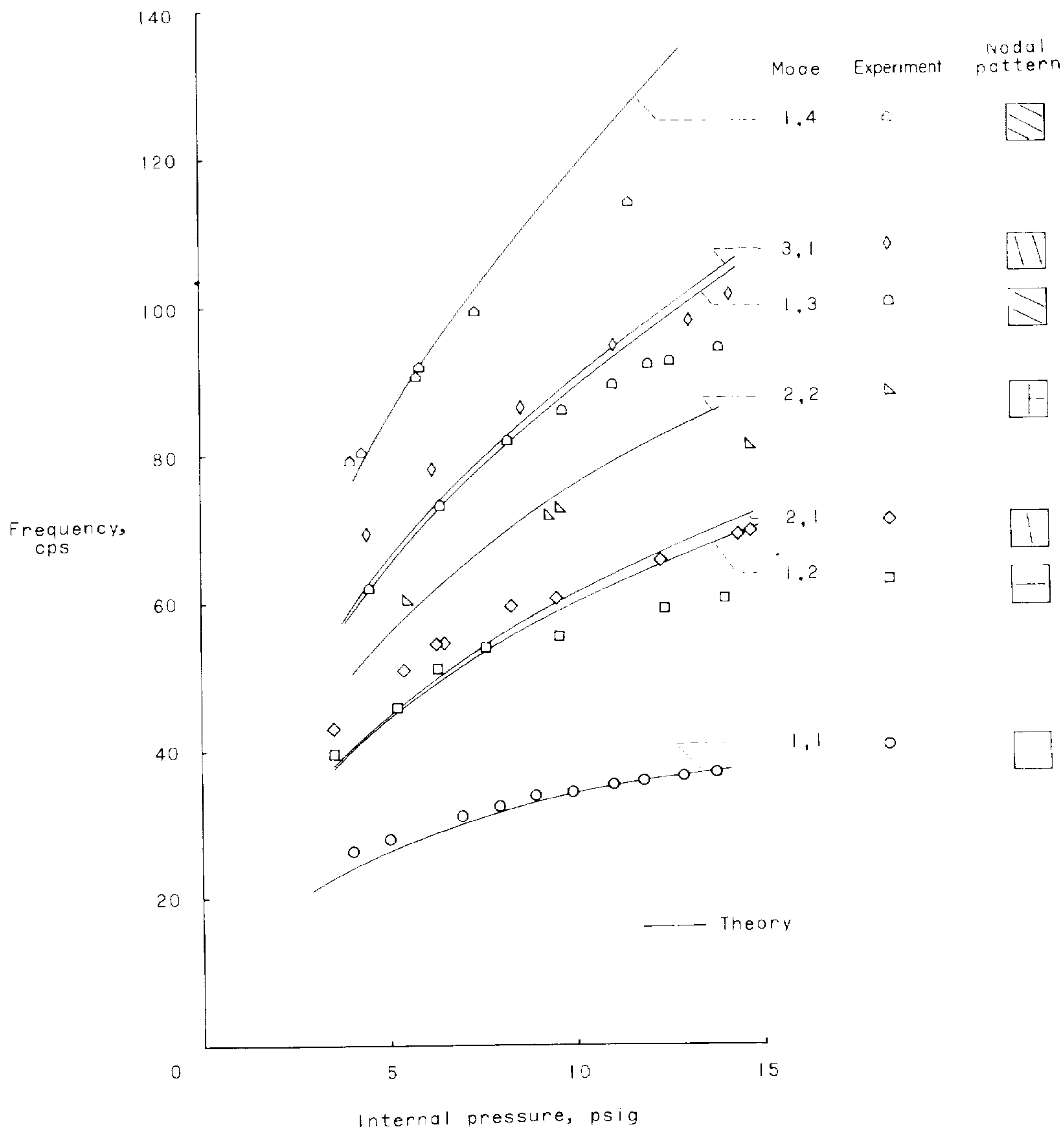

Figure 10.- Theoretical and experimental vibration frequencies as a function of internal pressure for several natural modes of vibration of simply supported inflatable plate.

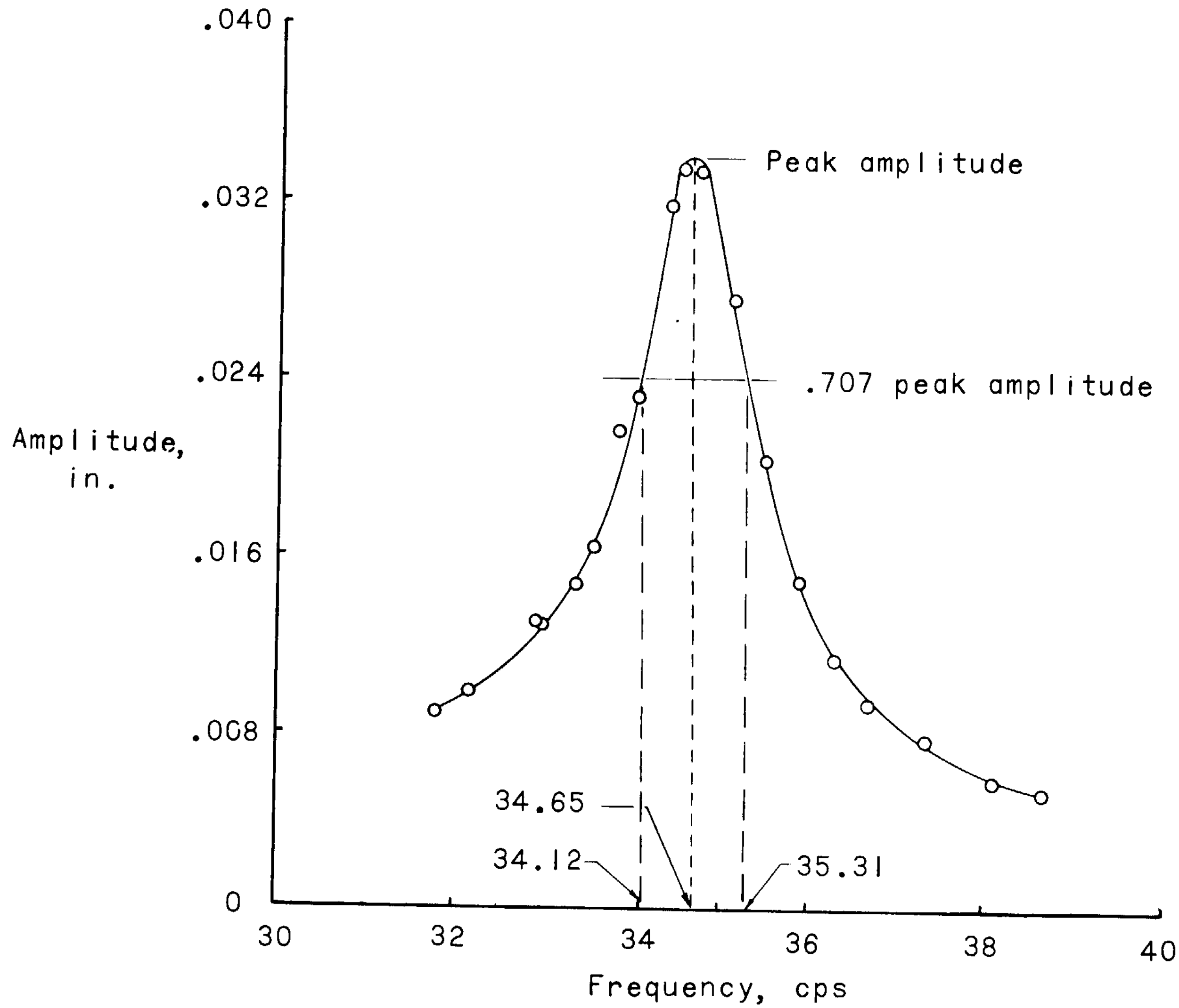

Figure 11.- Frequency-amplitude response curve for first mode of simply supported plate. Internal plate pressure = 9.4 psig.

L-1317

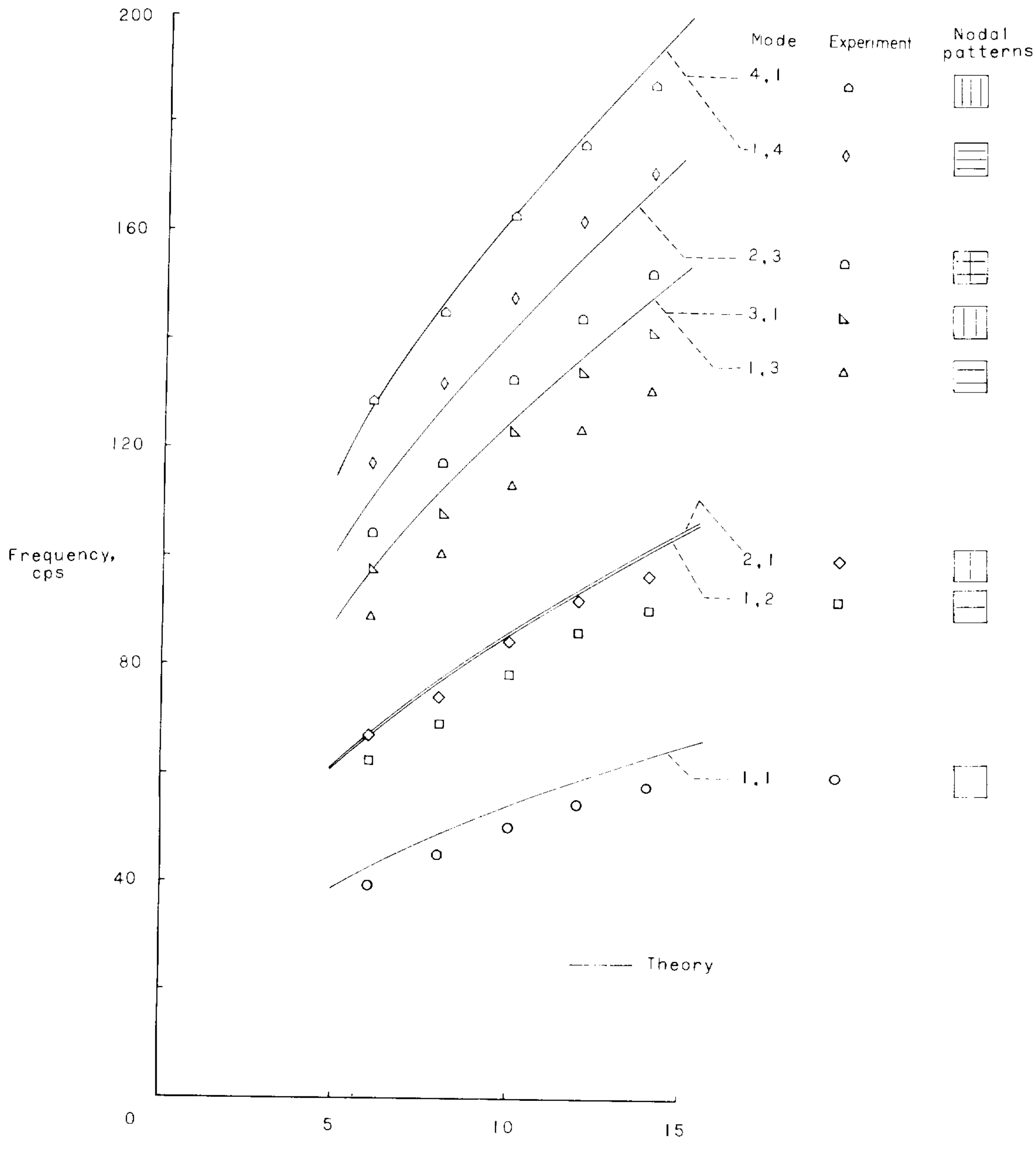

Figure 12.- Theoretical and experimental vibration frequencies plotted against internal pressure for several natural modes of vibration of clamped inflatable plate.

NASA TN D-931
National Aeronautics and Space Administration.
EXPERIMENTAL AND THEORETICAL DEFLECTIONS AND NATURAL FREQUENCIES OF AN INFLATABLE FABRIC PLATE. W. Jefferson Stroud. October 1961. 27p. OTS price, $0.75.
(NASA TECHNICAL NOTE D-931)

Static and vibration tests were performed on an inflatable square fabric plate supported on all edges. Clamped and simple-support boundary conditions were used in the tests. Lateral deflections and natural frequencies showed good agreement with calculations made using a linear small-deflection theory.

Copies obtainable from NASA, Washington

I. Stroud, W. Jefferson
II. NASA TN D-931

(Initial NASA distribution:
51, Stresses and loads;
52, Structures.)

NASA

NASA TN D-931
National Aeronautics and Space Administration.
EXPERIMENTAL AND THEORETICAL DEFLECTIONS AND NATURAL FREQUENCIES OF AN INFLATABLE FABRIC PLATE. W. Jefferson Stroud. October 1961. 27p. OTS price, $0.75.
(NASA TECHNICAL NOTE D-931)

Static and vibration tests were performed on an inflatable square fabric plate supported on all edges. Clamped and simple-support boundary conditions were used in the tests. Lateral deflections and natural frequencies showed good agreement with calculations made using a linear small-deflection theory.

Copies obtainable from NASA, Washington

I. Stroud, W. Jefferson
II. NASA TN D-931

(Initial NASA distribution:
51, Stresses and loads;
52, Structures.)

NASA

NASA TN D-931
National Aeronautics and Space Administration.
EXPERIMENTAL AND THEORETICAL DEFLECTIONS AND NATURAL FREQUENCIES OF AN INFLATABLE FABRIC PLATE. W. Jefferson Stroud. October 1961. 27p. OTS price, $0.75.
(NASA TECHNICAL NOTE D-931)

Static and vibration tests were performed on an inflatable square fabric plate supported on all edges. Clamped and simple-support boundary conditions were used in the tests. Lateral deflections and natural frequencies showed good agreement with calculations made using a linear small-deflection theory.

Copies obtainable from NASA, Washington

I. Stroud, W. Jefferson
II. NASA TN D-931

(Initial NASA distribution:
51, Stresses and loads;
52, Structures.)

NASA

NASA TN D-931
National Aeronautics and Space Administration.
EXPERIMENTAL AND THEORETICAL DEFLECTIONS AND NATURAL FREQUENCIES OF AN INFLATABLE FABRIC PLATE. W. Jefferson Stroud. October 1961. 27p. OTS price, $0.75.
(NASA TECHNICAL NOTE D-931)

Static and vibration tests were performed on an inflatable square fabric plate supported on all edges. Clamped and simple-support boundary conditions were used in the tests. Lateral deflections and natural frequencies showed good agreement with calculations made using a linear small-deflection theory.

Copies obtainable from NASA, Washington

I. Stroud, W. Jefferson
II. NASA TN D-931

(Initial NASA distribution:
51, Stresses and loads;
52, Structures.)

NASA